Steel and Composite Structures, *Vol. 21, No. 2 (2016) 323-342*
DOI: http://dx.doi.org/10.12989/scs.2016.21.2.323

Static strength of collar-plate reinforced tubular T-joints under axial loading

Yong-Bo Shao*

School of Mechatronic Engineering, Southwest Petroleum University, Xindu Avenue 8#, Chengdu, Sichuan Province, P.R. China

(*Received June 29, 2015, Revised December 08, 2015, Accepted April 04, 2016*)

Abstract. To study the effect of collar-plate reinforcement on the static strength of tubular T-joints under axial loading, fundamental research work is carried out from both experimental test and finite element (FE) simulation. Through experimental tests on 7 collar-plate reinforced and 7 corresponding un-reinforced tubular T-joints under axial loading, the reinforcing efficiency is investigated. Thereafter, the static strengths of the above 14 models are analyzed by using FE method, and it is found that the numerical results agree reasonably well with the experimental data to prove the accuracy of the presented FE model. Additionally, a parametric study is conducted to analyze the effect of some geometrical parameters, i.e., the brace-to-chord diameter ratio β, the chord diameter-to-chord wall thickness ratio 2γ, collar-plate thickness to chord wall thickness ratio τ_c, and collar-plate length to brace diameter ratio l_c/d_1, on the static strength of a tubular T-joint. The parametric study shows that the static strength can be greatly improved by increasing the collar-plate thickness to chord wall thickness ratio τ_c and the collar-plate length to brace diameter ratio l_c/d_1. Based on the numerical results, parametric equations are obtained from curving fitting technique to estimate the static strength of a tubular T-joint with collar-plate reinforcement under axial loading, and the accuracy of these equations is also evaluated from error analysis.

Keywords: tubular T-joint; collar-plate reinforcement; experimental tests; finite element simulation; static strength; parametric equations

1. Introduction

Welded steel circular hollow section joints and their reinforcements can be found in space structures, towers, bridges and offshore structures because of its light weight, high strength, ease of fabrication and fast construction. Generally, the stiffness of a hollow section tube in radial direction is much weaker than that of the tube in axial direction, especially when the tube is relatively thin. Therefore, the chord surface near the weld toe is the critical region, and failure generally initiates at this position in a tubular structure. To improve the bearing capacity of a tubular joint, the chord surface near the weld region is necessary to be strengthened or some other measures should be considered.

Besides strengthening methods, two other alternatives in the literature have been introduced. The first one is to use high strength steel to improve the bearing capacity of a tubular joint (Choi *et*

*Corresponding author, Professor, E-mail: ybshao@swpu.edu.cn

http://www.techno-press.org/?journal=scs&subpage=6 ISSN: 1229-9367 (Print), 1598-6233 (Online)

al. 2012). The second one is to use a bird-beak joint with a special placement for the cross section of the chord (Pena and Chacon 2014). For conventional tubular joints, there are several reinforcing methods reported in literature. These reinforcing methods can be classified into two types: inner reinforcement and outer reinforcement. The inner reinforcement places the stiffeners inside the chord near the brace/chord intersection, such as internal ring stiffening method (Thandavamoorthy *et al*. 1999, Gandhi *et al*. 2000, Zhang *et al*. 2004, Hamid and Esmaeil 2015, Hamid *et al*. 2015), inner plate reinforcement (Li *et al*. 2009, Shao *et al*. 2009, Chiew *et al*. 2012), chord thickness reinforcement (Jin and Shao 2010, Shao *et al*. 2011), and infilled-concrete reinforcement (Kim *et al*. 2014). The first two methods have been applied in various engineering structures, and a lot of researches have been conducted in this field. The chord thickness reinforcement is a relatively new method although it is more challenging in strengthening tubular structures in recent years. It is found both from experimental tests and numerical analyses that the static strength of a tubular joint can be improved greatly by inner reinforcement method. Because inner reinforcement method does not affect the appearance of joints, it can maintain the aesthetics of the structure. However, it is difficult to ensure welding quality due to its complex operating and constructing difficulty. For the outer reinforcement, the stiffeners are placed outside the chord, such as doubler-plate reinforcement (Fung *et al*. 1999, Hoon *et al*. 2001, Choo *et al*. 2004a, Yin *et al*. 2009, Chen *et al*. 2015, Wang *et al*. 2015, Gao *et al*. 2015), collar-plate reinforcement (Choo *et al*. 1998) and FRP reinforcement (Aguilera and Fam 2013, Lesani *et al*. 2013, Ghazijahani *et al*. 2015). The doubler-plate reinforcement can be found in various components in offshore platform structures. In literature, a series of studies can be found related to doubler-plate reinforced joints. The collar-plate reinforcement scheme has been proposed by Choo *et al*. (1998). Static strength of tubular T-joints reinforced with doubler- or collar-plates under axial loading is reported by Choo *et al*. (2005) and van der Vegte *et al*. (2005). It is found that significant strength enhancement can be obtained by providing appropriately proportioned doubler- or collar-plate. Static strength of collar-plate reinforced CHS X-joints loaded by in-plane bending was also investigated by Choo *et al*. (2004b). Similar conclusion can be obtained on the improvement of static strength. The collar-plate reinforcement can be more convenient for construction compared to other reinforcement methods. The most challenging advantage of this method is that it can be used for the on-site reinforcement during servicing time. However, other methods mentioned above can only be used in the design stage. Therefore, it has greater potential application, thus further study on this reinforcing method is needed.

Based on the above analyses, both experimental investigation and numerical simulation are carried out to investigate the behavior of tubular T-joints with collar plate reinforcement under axial compression or tension in this paper. Additionally, the effects of some principal geometric parameters on the static strength of the reinforced joints are evaluated. Finally, parametric equations are presented to predict the static strength of tubular T-joints with collar-plate reinforcement under axial loading.

2. Experimental program

2.1 Specimen details

Fig. 1 shows a typical collar-plate reinforced circular tubular T-joint. In a collar-plate reinforced tubular joint, the brace is firstly welded directly onto the chord surface by using penetrated weld, and a curved plate with a hole is then welded onto the chord surface and around

the brace. The collar-plate to the chord surface and the collar-plate to the brace are connected by using fillet weld. After welding, an ultrasonic technique is used to check the welding quality along the weld length. Some geometric parameters are illustrated in Fig. 1. For convenience, the quantity with a subscript "0" denotes a geometric parameter of the chord, and the quantity with a subscript "1" denotes a geometric parameter of the brace. Accordingly, a geometric parameter of the collar-plate is denoted by the quantity with a subscript "c". Some normalized parameters are used in the study to describe a tubular T-joint with collar-plate reinforcement, such as the brace-to-chord diameter ratio β, the chord diameter-to-chord wall thickness ratio 2γ, the brace-to-chord thickness ratio τ, collar-plate to chord wall thickness ratio τ_c, and collar-plate length to brace diameter ratio l_c/d_1.

The experimental program consists of 14 tests, including 7 collar-plate reinforced T-joints and 7 corresponding un-reinforced T-joints. The details of the specimens are summarized in Table 1. For comparison, the un-reinforced and the corresponding reinforced tubular T-joints have same geometric dimensions and material properties. Therefore, the specimens can be divided into seven

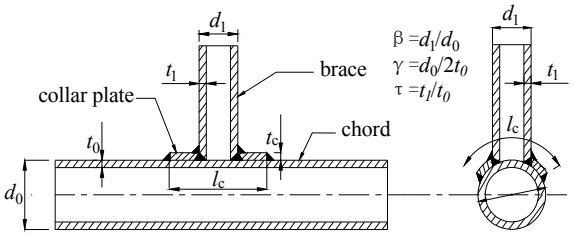

Fig. 1 A collar-plate reinforced tubular T-joint

Table 1 Details of specimens

Specimen	Type	d_0	d_1	t_0	t_1	l_0	l_1	t_c	l_c	β	2γ	Brace loading
1#	Un-reinforced	203	50	6	6	2000	300	-	-	0.246	33.83	compression
2#	Reinforced	203	50	6	6	2000	300	6	75	0.246	33.83	compression
3#	Un-reinforced	203	50	6	6	2000	300	-	-	0.246	33.83	tension
4#	Reinforced	203	50	6	6	2000	300	6	75	0.246	33.83	tension
5#	Un-reinforced	203	90	6	6	2000	400	-	-	0.443	33.83	compression
6#	Reinforced	203	90	6	6	2000	400	6	135	0.443	33.83	compression
7#	Un-reinforced	203	90	6	6	2000	400	-	-	0.443	33.83	tension
8#	Reinforced	203	90	6	6	2000	400	6	135	0.443	33.83	tension
9#	Un-reinforced	203	140	6	6	2000	500	-	-	0.690	33.83	compression
10#	Reinforced	203	140	6	6	2000	500	6	210	0.690	33.83	compression
11#	Un-reinforced	203	140	6	6	2000	500	-	-	0.690	33.83	tension
12#	Reinforced	203	140	6	6	2000	500	6	210	0.690	33.83	tension
13#	Un-reinforced	180	50	8	6	2000	300	-	-	0.278	22.50	compression
14#	Reinforced	180	50	8	6	2000	300	8	75	0.278	22.50	compression

Notes: All dimensions are measured and in mm. t_c = thickness of collar-plate. l_c = length of collar-plate

Table 2 Material properties

Member	Diameter (mm)	Yield stress (N/mm^2)	Tensile stress (N/mm^2)	Elongation
Chord	203	321	480	25.4%
Chord	180	324	480	22.5%
Collar-plate	203	348	516	26.8%
Collar-plate	180	332	476	20.9%
Brace	50	389	576	16.2%
Brace	90	380	550	17.1%
Brace	140	318	483	24.7%

groups, and each group includes an un-reinforced specimen and a corresponding collar-plate reinforced specimen. The collar plate t_c has the same thickness with the chord, and the length of the collar plate l_c is kept as 1.5 times of the brace diameter ($l_c = 1.5\ d_1$) both in the longitudinal direction and in the circumferential direction.

The material properties of the specimens measured from tensile coupon tests are summarized in Table 2. It is found that the material properties of the chord are basically same as those of the collar-plates.

2.2 Test setup and loading scheme

Fig. 2 shows general arrangement of the test setup for tubular T-joint specimens. The specimen is pinned at both ends of the chord, and an axial load is applied at the brace end. The magnitude of the axial load produced by the instrument is ±500 kN, and the magnitude of the axial displacement at the brace end is ±75 mm. During the test, the applied load together with the corresponding displacement at the brace end can be recorded automatically from Data Acquisition System installed in the computer. To obtain the deformation of the chord member, an LVDT was placed under the bottom of the chord in the mid-span of the specimen to measure the vertical displacement of the bottom of the chord, as shown in Fig. 2. The deformation of the specimen is then defined as the difference between the displacements measured from the LVDT and the brace end. It is assumed that the axial compressive or tensile deformation of the brace is ignorable compared to the radial deformation of the chord.

Fig. 2 Test setup

There are two schemes for loading application: one is displacement controlling method, and the other one is load controlling method. If load controlling method is used, it is difficult to control the loading step when the specimen is in plastic state because a large deformation may occur even if only a small loading increment is applied after the specimens yield. Additionally, it is impossible to increase the load further after the load reaches the peak point in loading controlling method if there is a remarkable loading drop after the peak load in the load-deformation curve. Therefore, the displacement controlling method is used in the test. In each test, the brace end displacement is applied at a rate of 1 mm/min in the linear loading range, and 2 mm/min after the yield stage begins.

2.3 Experimental results

2.3.1 Specimens under axial compression

Figs. 3(a)-(d) show the deformation of the un-reinforced specimens after testing. Localized chord indentation around the brace/chord intersection is observed in each of the three un-reinforced joints with a smaller value of brace-to-chord diameter ratio β as shown in Figs. 3(a), (b) and (d). Meanwhile, the chord bottom remains relatively approximately straight for the three specimens. In overall, the failure modes of the 4 un-reinforced specimens can be generalized as local failure on the chord surface along the weld toe, which verifies the fact that the stiffness of the chord in radial direction is much weaker than that of the brace in axial direction. Generally, when the value of β is small, the axial compression transferred from the brace to the chord is acted on a relatively smaller area of the chord surface, and local yielding on the chord surface around the brace/chord intersection occurs more easily, which is verified through the observation of the failure mode of specimen 1# as shown in Fig. 3(a). However, for a tubular T-joint with a large value of β, local yielding on the chord surface is not so pronounced, as shown in Fig. 3(c). For the specimen in Fig. 3(d), the radial stiffness of the chord is big because the thickness of the chord is large, and such big radial stiffness of the chord makes the local deformation around the brace/chord intersection not remarkable although the value of β is small.

(a) 1# (b) 5# (c) 9# (d) 13#

Fig. 3 Deformation of the un-reinforced specimens

(a) 2# (b) 6# (c) 10# (d) 14#

Fig. 4 Deformation of collar-plate reinforced specimens


(a) 3#


(b) 7#


(c) 11#

Fig. 5 Final failure mode of un-reinforced specimens

For the collar-plate reinforced specimens (2#, 6#, 10# and 14#), Figs. 4(a)-(d) show the deformation around brace/chord intersection after testing. When the parameter β has a small value, local yielding is also the main failure mode. As the collar-plate can increase the stiffness of the chord in radial direction, local yielding failure moves to the region along the edge of the collar-plate on the chord surface. When the value of β becomes larger, failure modes of collar-plate reinforced specimens 6# and 10# are changed from local yielding around the brace/chord intersection to the yielding of the chord along the collar-plate, which can be seen in Figs. 4(b) and 4(c) in which the flexural deformation of the chord is also observed to be pronounced.

2.3.2 Specimens under axial tension

Figs. 5(a)-(c) show the final failure modes of the un-reinforced specimens under axial tension. When the value of β is small, localized chord bulge around the brace/chord intersection is observed in the un-reinforced specimens under brace tension, while the chord bottom remains relatively straight as shown in Figs. 5(a) and (b), which indicates that the deformation is concentrated locally around the weld and the flexural deformation of the chord is very slight. Therefore, the failure modes can be generalized as local yielding on the chord surface along the weld toe. However, the specimen failed due to flexural failure of the chord when the parameter β has a large value because the chord behaves much like a bending beam observed in the experimental test as seen in Fig. 5(c).

Figs. 6(a)-(c) show the final failure modes of collar-plate reinforced specimens under axial tension. When the parameter β has a small value, local yielding is also the failure mode of the specimen with the collar-plate reinforcement as seen in Fig. 6(a). However, such local yielding moves outward to the weld toe along the edge of the collar-plate. The chord surface at the brace/chord intersection protrudes outward and the chord bottom remained relatively straight to


(a) 4#


(b) 8#


(c) 12#

Fig. 6 Final failure mode of collar-plate reinforced specimens

indicate that the flexural deformation of the chord is still minor. Flexural yielding of the chord is the final failure mode when the value of β becomes larger, which can be found for specimens #8 and #12 shown in Figs. 6(b) and 6(c). Obvious plastic flexural deformation of the chord caused by brace tension can be observed.

3. Finite element analyses

3.1 Finite element model

To investigate the static strength of tubular T-joints with different geometries or different sizes of the collar-plate, experimental test usually has limitations due to the high cost and time consuming. Finite element (FE) method is a useful tool to offer an attractive and cheaper alternative to carry out numerical analyses for amounts of models. However, the accuracy and the reliability of the FE results must be verified against benchmark test. It is a suitable way to evaluate the FE model by comparing the numerical results with the experimental results.

The element types, material properties, boundary conditions and the contact between the collar-plate and the chord surface have significant effect on the accuracy of the FE results. FE software ANSYS is used in this study to build the numerical models of the un-reinforced and the collar-plate reinforced tubular T-joints. 3-D 20-node solid elements (solid 95) are used in the FE models. To guarantee the convergence and to improve the computational efficiency, the mesh around the brace/chord intersection is refined due to high gradient stresses in this region while a relatively coarse mesh is used far away from the brace/chord intersection. Contact interaction plays an important role in the load transferring mechanism between the collar-plate and the chord. Contact interaction occurs between the bottom surface of the collar-plate and the outer surface of the chord wall, and a deformable-to-deformable contact is thus defined using a "master-slave" strategy (Hoon *et al*. 2001). The bottom of the collar-plate is defined as master surface using targe170 element, and the outer surface of the chord wall is defined as slave surface using conta174 element. The FE mesh of a typical tubular T-joint with collar-plate reinforcement is shown in Fig. 7. Preliminary FE analyses show that such a mesh density is able to produce results with good convergence.

The effect of the weld around the brace/chord intersection and the effect of the residual stress on the static strength of the tubular joints are not considered in the FE analyses. For the steel material, isotropic hardening property is used to define the nonlinear property of the material after yielding. The tangential modulus of the stress-strain curve after yielding point is obtained from experimental test. The elastic modulus is 200 GPa, and the Poisson's ratio is 0.3.

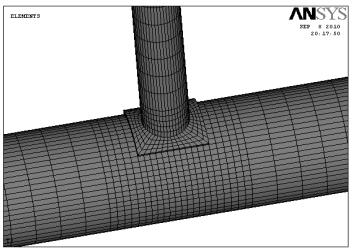

Fig. 7 FE mesh of a reinforced T-joint

For the boundary conditions, both ends of the chord are pined to simulate the actual constraints in experimental test. Only vertical constraint at the brace end is released by restricting the degrees of freedom in other directions. Increment of axial displacement at the brace end is used to produce axial loading to the tubular joints.

Using the above FE modelling method, all of the specimens tabulated in Table.1 are analyzed, and the numerical results are compared with the experimental results.

3.2 Comparison of deformation between experimental and numerical results

Figs. 8(a)-(h) show the FE simulated deformation of the specimens under axial compression, and Figs. 9(a)-(f) show the FE results of the specimens under axial tension. The FE simulations are very close to the experimental results as shown in Figs. 3-6. The comparison shows that the FE modeling can provide reliable prediction on the failure modes of both un-reinforced and collar-plate reinforced tubular T-joints under axial compression or tension.

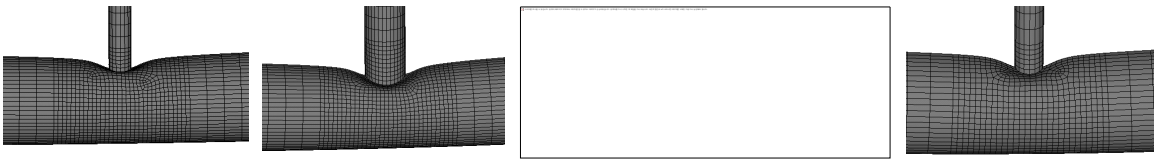

(a) 1# (b) 5# (c) 9# (d) 13#

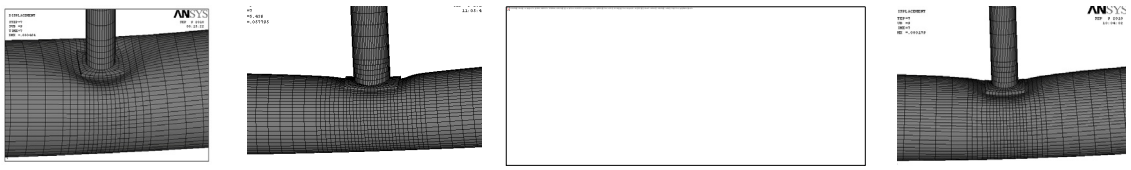

(e) 2# (f) 6# (g)10# (h) 14#

Fig. 8 Deformation of the specimens (compression)

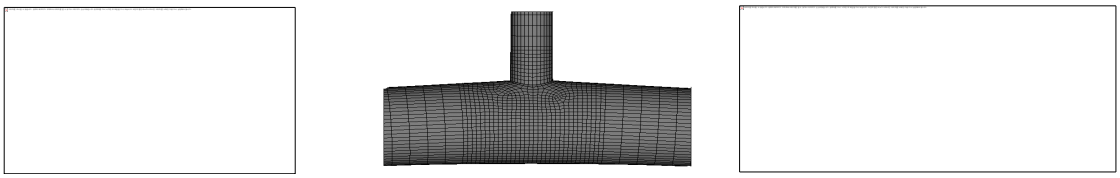

(a) 3# (b) 7# (c) 11#

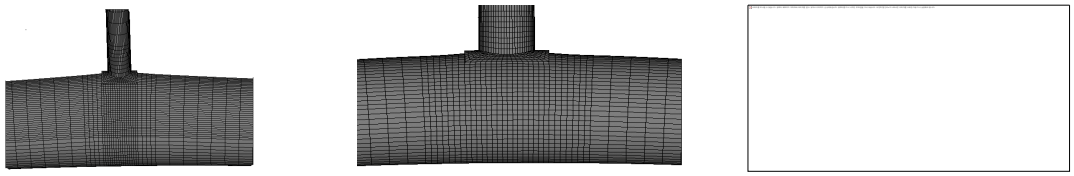

(d) 4# (e) 8# (f) 12#

Fig. 9 Deformation of the specimens (tension)

3.3 Comparison of load-deformation curves

According to the experimental data, the load-deformation curves of the specimens in the loading process are obtained. There are several methods to define the static strength of a tubular joint from the load-deformation curve. The peak load in the load-deformation curves is defined as the static strength when the load–deformation curve has a clear decreasing stage after a peak point. However, this method is not applicable if there is no pronounced peak point in the load-deformation curve. In this case, the deformation limit proposed by Lu *et al*. (1994) is selected to define the ultimate load. The corresponding load at a chord deformation of 3%d_0 (d_0 is the chord diameter) is defined as the static strength of the tubular joint.

Figs. 10(a)-(d) show the load-deformation curves of the tubular T-joints under axial compression obtained from experimental test and FE simulation respectively. RS and URS in the figures denote reinforced specimen and un-reinforced specimen respectively. The static strengths of the collar-plate reinforced specimens are found to be improved significantly because the peak loads at the load-deformation curves are higher. The static strength of the collar-plate reinforced specimen #2 is increased by 22.2% compared to that of the un-reinforced specimen #1, as shown

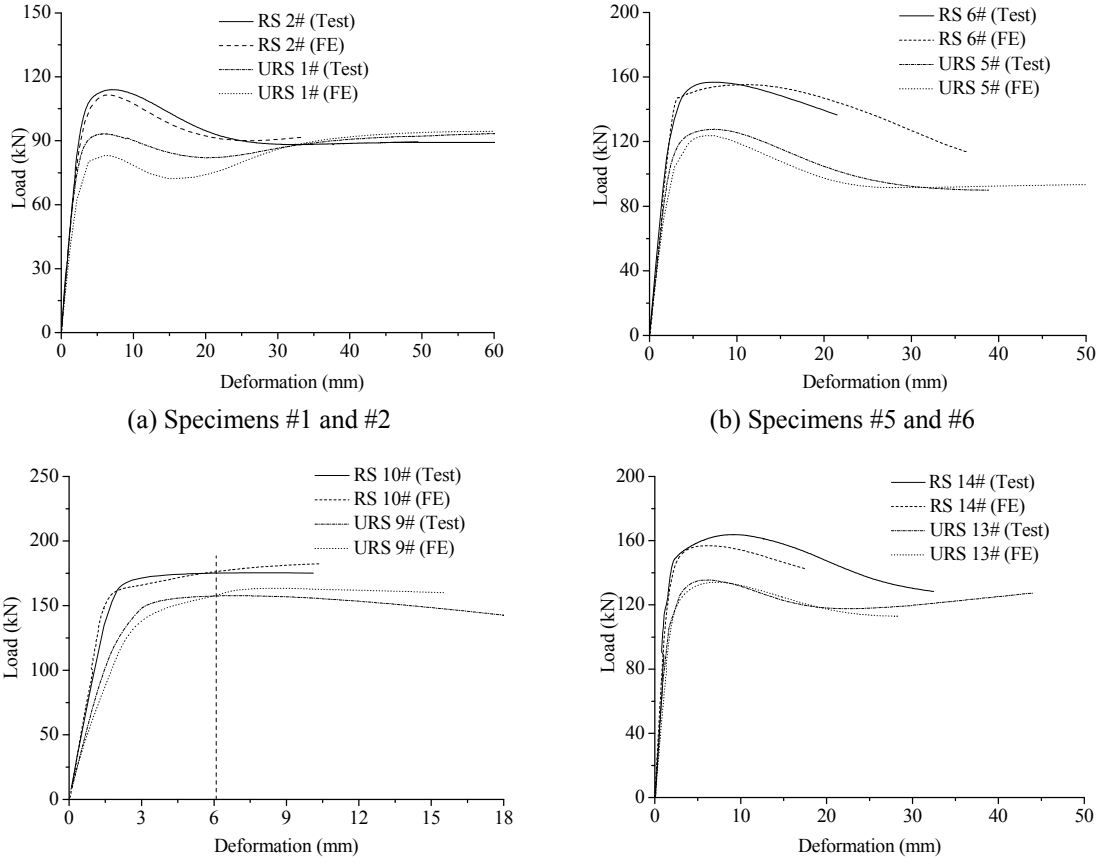

(a) Specimens #1 and #2

(b) Specimens #5 and #6

(c) Specimens #9 and #10

(d) Specimens #13 and #14

Fig. 10 Load-deformation curves under axial compression

in Fig. 10(a). The collar-plate reinforced specimen #6 has a strength enhancement of 21.7% compared to the un-reinforced specimen #5, which can be observed from Fig. 10(b). As shown in Fig. 10(c), because no pronounced peak loads can be found in the load-deformation curve, the static strength is determined from Lu's limit of $3\%d_0$. It can be observed that the reinforced specimen #10 has a relatively little strength enhancement of 12.1% compared to the un-reinforced specimen #9. Compared to the un-reinforced specimen #13, a strength enhancement of 22.6% of specimen #14 with collar-plate reinforcement is found in the Fig. 10(d).

The improvement of the static strength of a tubular T-joint is dependent much on the value of parameter β. When the value of β is small, the static strength of a collar-plate reinforced specimen can be improved greatly, as shown in Figs. 10(a), 10(b) and 10(d). However, when the value of β is big, the effect of the collar-plate reinforcement on the improvement on the static strength is relatively slight as shown in Fig. 10(c).

Figs. 11(a)-(c) show the load-deformation curves of the specimens under axial tension, and they are obtained from experimental test and FE simulation respectively. The static strengths of the collar-plate reinforced specimens are also improved. Similarly, when parameter β has a small value, the static strength can be improved significantly (as shown in Figs. 11(a) and 11(b)), and the

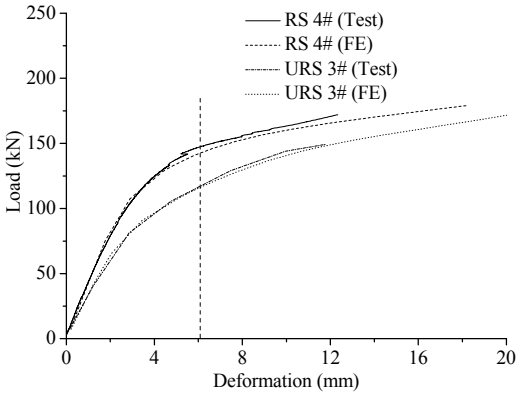

(a) Specimens #3 and #4

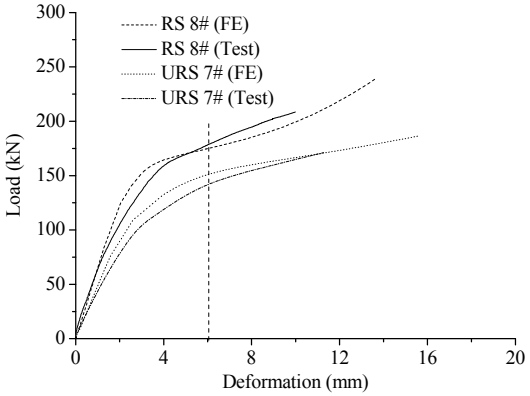

(b) Specimens #7 and #8

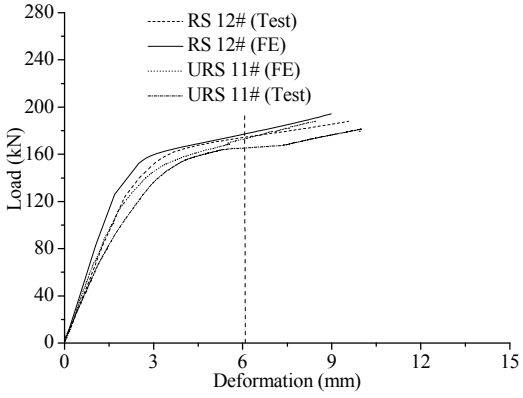

(c) Specimens #11 and #12

Fig. 10 Load-deformation curves under axial tension

Table 3 Comparison between experimental and numerical ultimate loads

Specimen	Type	P_t (kN)	P_f (kN)	P_f/P_t
1#	Un-reinforced	93.27	83.14	0.89
2#	Reinforced	114.01	111.60	0.98
3#	Un-reinforced	117.22	116.32	0.99
4#	Reinforced	147.46	142.54	0.97
5#	Un-reinforced	127.63	123.68	0.97
6#	Reinforced	155.44	156.78	1.01
7#	Un-reinforced	142.66	151.64	1.06
8#	Reinforced	178.96	175.33	0.98
9#	Un-reinforced	156.62	157.65	1.01
10#	Reinforced	176.34	175.15	0.99
11#	Un-reinforced	165.32	177.36	1.07
12#	Reinforced	173.30	174.52	1.01
13#	Un-reinforced	134.11	135.56	1.01
14#	Reinforced	163.81	156.92	0.96

reinforcing efficiency is not pronounced when the value of β is large (as shown in Fig. 11(c)). The static strengths of the collar-reinforced specimens #4, #8 and #12 are increased by 25.7%, 25.4% and 4.8% respectively compared to the static strengths of the corresponding un-reinforced specimen #3, #7 and #12. The reinforced specimen #12 has a slight strength enhancement of 4.8% compared to the specimen #11 because the reinforced specimen has a big value of β and the radial stiffness of the chord around the brace/chord intersection is improved greatly. The improved radial stiffness of the chord causes local yielding around the brace/chord intersection to occur later than the flexural failure of the chord.

The static strengths of all the tested specimens obtained from experimental tests and numerical simulations are summarized in Table 3. In Table 3, P_f and P_t are static strengths of a specimen obtained from FE simulation and experimental test respectively. From Figs. 10-11 and Table 3, it can be found that the numerical simulation can provide accurate estimation. Except for specimen 1#, the relative errors between the two results are all smaller than 10% for other specimens, which indicates that the FE simulation is reliable in predicting the static strength of both un-reinforced and collar-plate reinforced tubular T-joints.

4. Parametric study

To investigate the efficiency of collar-plate reinforcement on improving the static strength of tubular T-joints with different geometric dimensions, a parametric study is conducted by using FE simulation. Six parameters, including the brace-to-chord diameter ratio β, the chord diameter-to-thickness ratio 2γ, the chord thickness t_0, thickness ratio τ_c between collar-plate and chord wall, collar-plate length to brace diameter ratio l_c/d_1 and the type of loading (compression or tension), are considered. For each parameter, four different values are selected, and the values of the parameters are tabulated in Table 4.

Table 4 Values of parameters

β	0.2,0.4,0.6,0.8
γ	12,18,24,30
t_0	5,8,12,15
τ_c	0.8,1.0,1.2,1.5
l_c/d_1	1.5,1.75,2.0,2.5

In the FE simulation, a half FE model for a tubular T-joint is analyzed due to the symmetry of the geometry, the loading conditions and the boundary conditions. For each FE model, the value of the chord length-to-radius ratio α ($2l_0/d_0$) is fixed to be 15, and the brace length is four times of the brace diameter ($l_1 = 4d_1$). The brace-to-chord thickness ratio τ is fixed to be 1.0. The collar-plate is selected to be a square plate. However, when β and l_c/d_1 are big, the length of the collar-plate exceeds half of the perimeter of the chord section, and the collar-plate is rectangular. In this case, the width of the collar-plate is limited to half of the perimeter of the chord tube.

The elastic-perfectly plastic model for the stress-strain relationship is used in the numerical analysis. The yield stress of the steel material used for the collar-plate reinforced T-joints is 235 N/mm^2. The modulus of elasticity is 206 GPa, and the Poisson's ratio is 0.3. For the boundary conditions, one end of the chord is hinged, and the other end is simulated as a roller to ensure that no initial axial stress in the chord. Only axial displacement at the brace end is allowed.

4.1 Failure mode

For tubular T-joints subject to axial compression, Figs. 12(a)-(d) show the typical failure modes of some selected collar-plate reinforced models with τ_c has a constant value of 1.0. Four failure modes are observed from the FE simulations on the models in the parametric study. When the value of l_c/d_1 is small, especially the parameter β also has a small value, the failure mode can be generalized as local yielding on the chord surface at the weld toe along the collar-plate edge, as shown in Fig. 12(a). In this failure mode, the collar-plate has almost no flexural deformation compared to the chord surface around it. If the collar-plate is longer, as shown in Fig. 12(b), it has a pronounced flexural deformation together with the chord surface around it. The collar-plate and the chord surface fail together in this case. The third failure mode is illustrated in Fig. 12(c), in which it is clear that local yielding moves to the chord surface at the edge of the collar-plate. The chord almost is in a straight line to indicate that no pronounced flexural deformation occurs in the chord. However, flexural failure of the chord becomes dominant in a collar-plate reinforced tubular T-joint when β has a large value, as shown in Fig. 12(d).

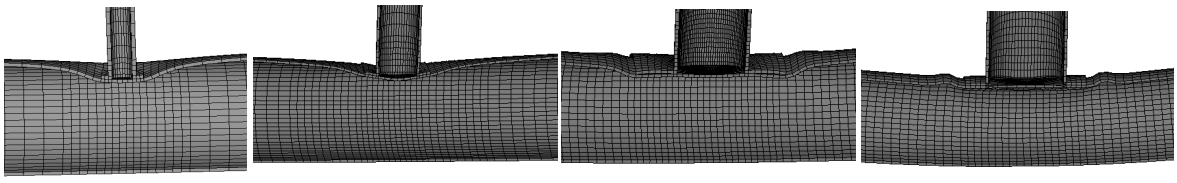

(a) $\beta = 0.2$, $l_c/d_1 = 1.5$ (b) $\beta = 0.4$, $l_c/d_1 = 2.0$ (c) $\beta = 0.6$, $l_c/d_1 = 2.0$ (d) $\beta = 0.8$, $l_c/d_1 = 1.5$

Fig. 12 Deformation of FE models under axial compression ($t_0 = 5$ mm)

For tubular T-joints subject to axial tension, three typical failure modes can be found. When parameter β has a very small value, the brace yields before the joint as shown in Fig. 13(a). When l_c/d_1 has a relatively small value as shown in Figs. 13(b)-(c), pronounced plastic deformation can be observed in the bottom of the chord at the mid-span. However, with a large value of l_c/d_1, as shown in Fig. 13(d), flexural failure of the chord occurs at the two edges of the collar-plate in its length direction.

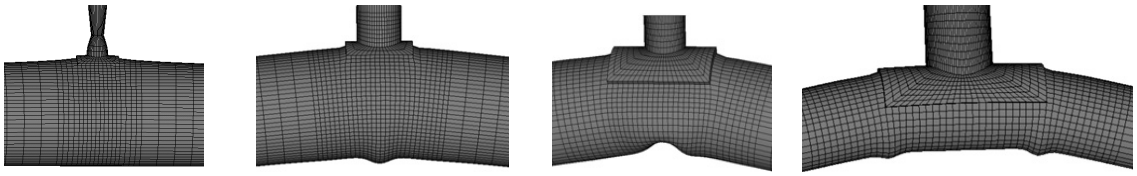

(a) $\beta = 0.2$, $l_c/d_1 = 1.5$ (b) $\beta = 0.4$, $l_c/d_1 = 2.0$ (c) $\beta = 0.4$, $l_c/d_1 = 2.5$ (d) $\beta = 0.8$, $l_c/d_1 = 2.5$

Fig. 13 Deformation of FE models under axial tension (t_0 = 5 mm)

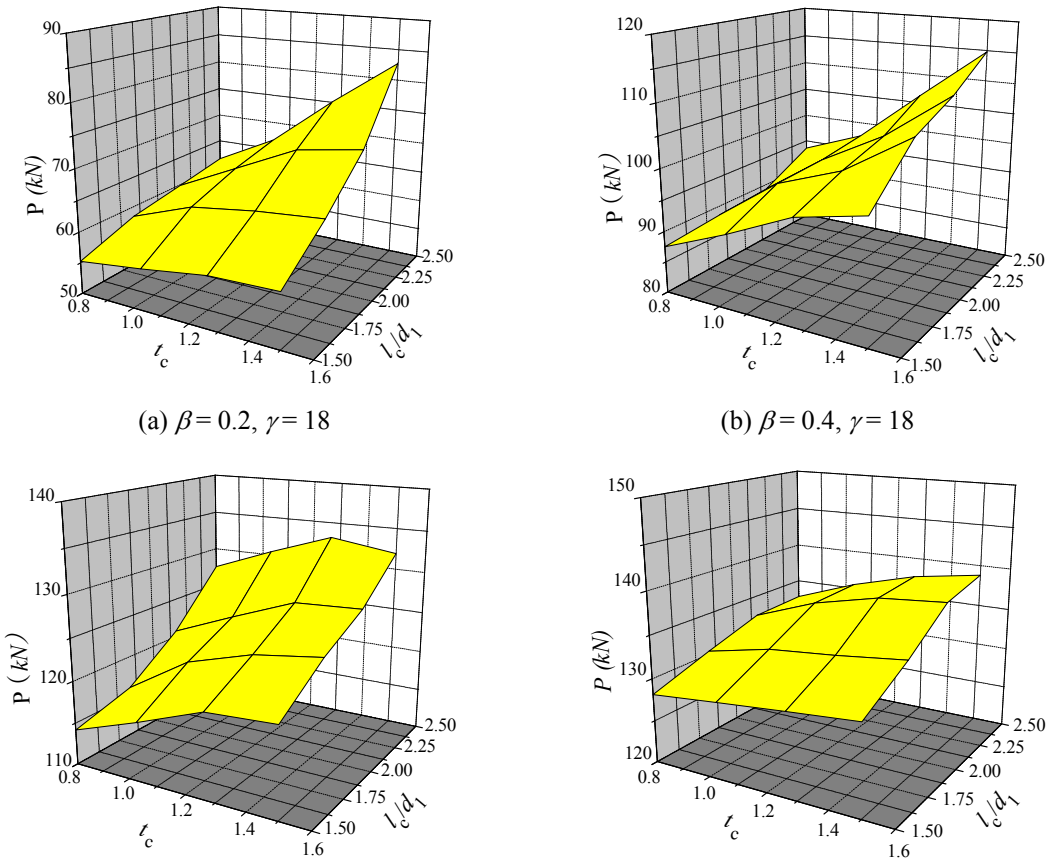

(a) $\beta = 0.2$, $\gamma = 18$ (b) $\beta = 0.4$, $\gamma = 18$

(c) $\beta = 0.6$, $\gamma = 18$ (d) $\beta = 0.8$, $\gamma = 18$

Fig. 14 Effect of τ_c and l_c/d_1 on static strength (compression)

4.2 Reinforcing efficiency of collar-plate on improving static strength

Figs. 14(a)-(d) show the effect of l_c/d_1 and τ_c on the static strength of tubular T-joints under axial compression when β has different values. For a tubular T-joint with small value of β, the effect of τ_c on the static strength is inefficient when l_c/d_1 has a small value. However, with the increase of the value of l_c/d_1, the effect of τ_c on the static strength becomes remarkable. It is more effective to improve the static strength by increasing the collar-plate thickness t_c when l_c/d_1 exceeds a certain value, as shown in Fig. 14(a). This phenomenon is produced because the failure mode is local yielding on the chord surface along the weld toe when β has a small value. A relatively small value of t_c can provide enough stiffness of chord in radial direction when l_c/d_1 is small, and thus it has a little effect to increase the value of τ_c to increase the static strength. However, for a joint with a large value of l_c/d_1, the stiffness of the collar-plate is not big enough to resist the chord deformation when t_c only has a small value, and in this case the static strength can be improved significantly by increasing the value of t_c. For a tubular T-joint with a medium value of β, as shown in Fig. 14(b), the static strength increases with the increase of τ_c and l_c/d_1, and the value of τ_c has an approximately linear relationship in improving the static strength. Furthermore, it is not effective to increase the value of l_c/d_1 to improve the static strength when τ_c is less than 1.0.

When β becomes larger, as shown in Fig. 14(c), the static strength of the collar-plate reinforced tubular T-joints can be still improved significantly by increasing the value of l_c/d_1, and the static strength increases roughly linearly with the increase of τ_c. However, the static strength has no increase when τ_c is bigger than a certain value (for example, $\tau_c \geq 1.2$ in Fig. 14(c)), which implies that it is ineffective to improve the static strength by increasing the thickness of the collar-plate in this case. When β has a very large value (for example, $\beta = 0.8$ in Fig. 14(d), it is almost ineffective to increase the value of τ_c to increase the static strength. Similarly, the static strength has an insignificant improvement by increasing the value of l_c/d_1. In this case, the failure mode of the collar-plate reinforced tubular T-joints varies from local yielding to flexural yielding of the chord. Because failure does not occur around the edges of the collar-plate (local yielding), increasing the dimensions of the collar-plate (τ_c and l_c/d_1) has little effect to improve the static strength.

For tubular T-joints under axial tension, the effect of l_c/d_1 and τ_c on the static strength has same conclusion, as shown in Figs. 15(a)-(d), and the reinforcing efficiency of parameters l_c/d_1 and τ_c on

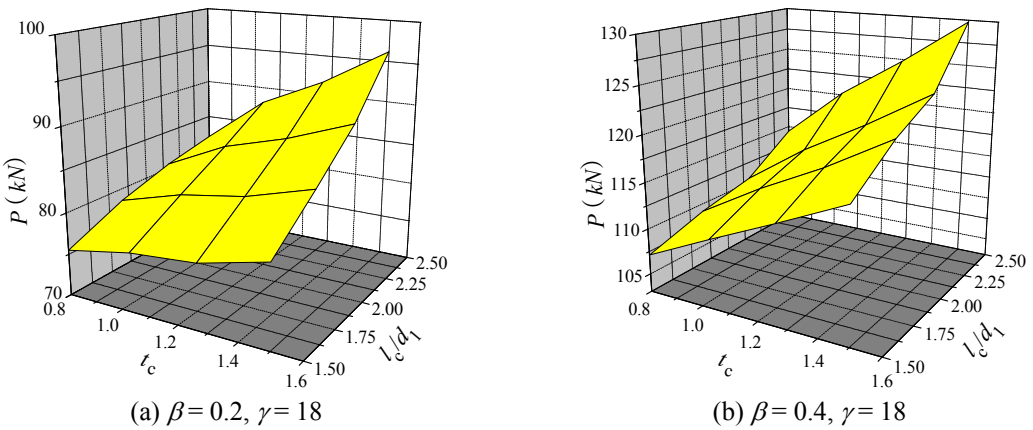

(a) $\beta = 0.2$, $\gamma = 18$ (b) $\beta = 0.4$, $\gamma = 18$

Fig. 15 Effect of τ_c and l_c/d_1 on static strength (tension)

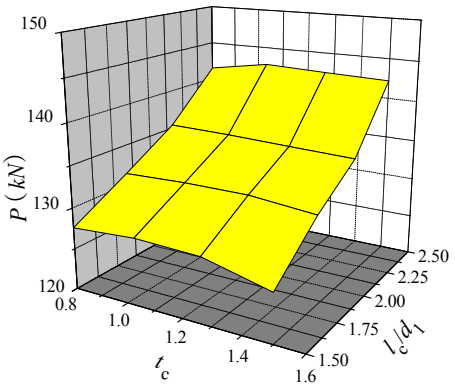

(c) $\beta = 0.6$, $\gamma = 18$

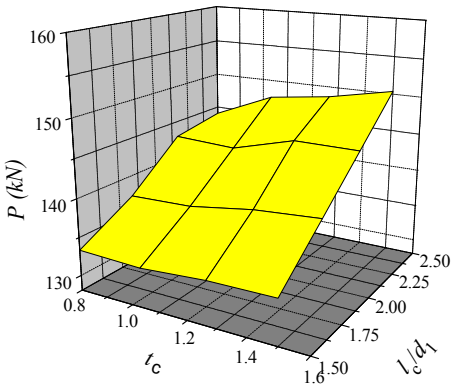

(d) $\beta = 0.8$, $\gamma = 18$

Fig. 15 Continued

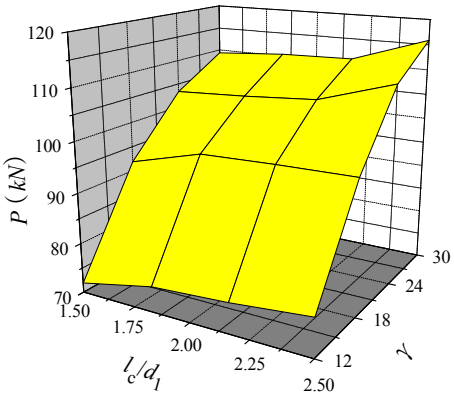

(a) $\beta = 0.2$, $\tau_c = 1.0$ (compression)

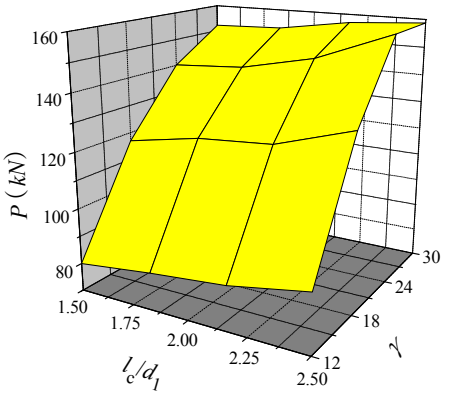

(b) $\beta = 0.6$, $\tau_c = 1.0$ (compression)

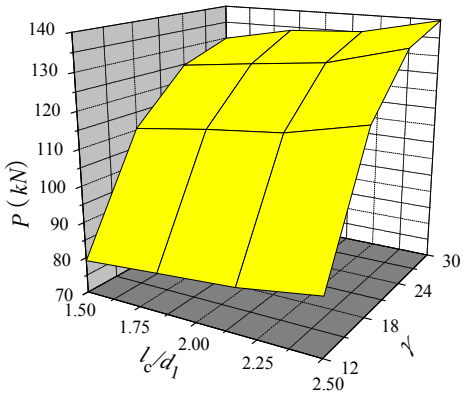

(c) $\beta = 0.4$, $\tau_c = 1.0$ (tension)

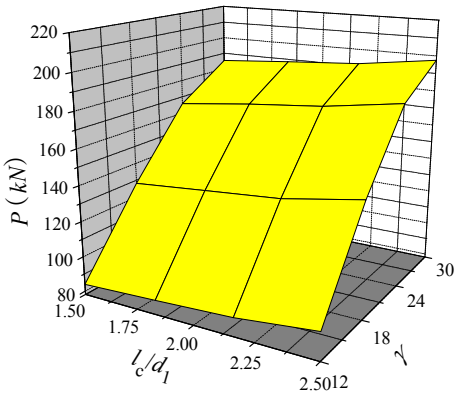

(d) $\beta = 0.6$, $\tau_c = 1.0$ (tension)

Fig. 16 Effect of γ on the bearing capacity ($t_0 = 5$ mm)

improving the static strength of tubular T-joints is consistent for both loading cases: compression and tension.

Figs. 16(a)-(d) show the effect of γ on improvement efficiency of the static strength of tubular T-joints under compression or tension. It can be observed that the static strength can be improved significantly by increasing the value of γ. It is because parameter γ denotes a ratio of radius to thickness for the chord, and a large value of γ indicates that the chord radius is very large compared to the chord thickness. Such large value of γ causes the flexural stiffness of the chord wall to be very weak, and a collar-plate reinforcement is then very efficient to increase the flexural stiffness of the chord wall. An improved flexural stiffness of the chord wall is effective to increase the static strength of the tubular T-joints. However, the reinforcing efficiency decreases with the increase of γ.

5. Parametric equations for predicting static strengths of collar-plate reinforced T-joints under axial loading

Through the above parametric study, the influences of various parameters on the static strength are obtained, and a set of parametric equations for predicting the static strength of tubular T-joints with collar-plate reinforcement under axial compression or tension are proposed by using curve fitting technique.

The static strength P of collar-plate reinforced CHS T-joints under axial compression is expresses as follow 0.929

$$P = 0.929\mu\left(\kappa\tau_c' - 0.1648\right)\beta_c f_y t^2 \tag{1}$$

where

$$\begin{aligned}
&\kappa = \left(0.3476 - 0.0165\beta\right)\left(2\gamma\right)^{0.0326} \\
&\mu = 2.267 + 0.334 l_c / d_1 \\
&\tau_c' = 0.4556 + 0.0056\tau_c \\
&\beta_c = 0.059 + 1.083\beta
\end{aligned} \tag{2}$$

The static strength P of collar-plate reinforced CHS T-joints under axial tension is expresses as follow

$$P = 1.0715\mu\left(\kappa\tau_c' - 0.1214\right)\beta_c f_y t^2 \tag{3}$$

where

$$\begin{aligned}
&\kappa = \left(0.3053 - 0.023\beta\right)\left(\gamma\right)^{0.0805} \\
&\mu = 1.583 + 0.1716 l_c / d_1 \\
&\tau_c' = 0.3617 + 0.00387\tau_c \\
&\beta_c = 0.102 + 1.2506\beta
\end{aligned} \tag{4}$$

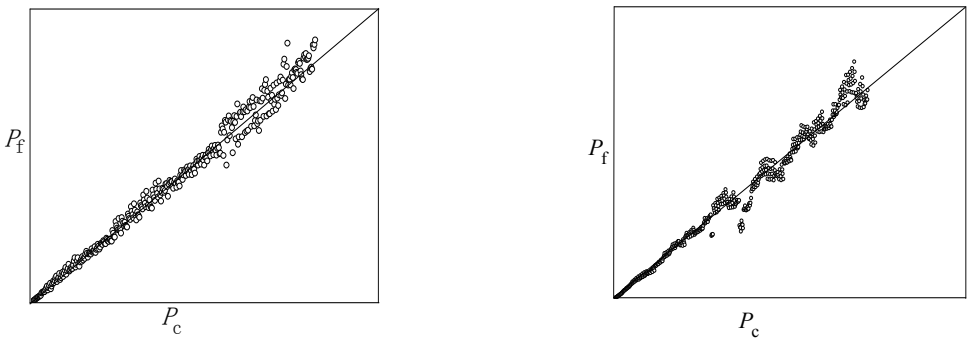

(a) Compression (b) Tension

Fig. 17 Comparison between predicated and FE results

To evaluate the accuracy of the above parametric equations in predicting the static strength of collar-plate reinforced tubular T-joints, the predicted results of all the models in the parametric study from Eqs. (1)-(4) are compared with the corresponding FE results. Figs. 17(a)-(b) show the comparison, where P_f represents the static strength obtained from FE simulation and P_c denotes the static strength calculated from Eqs. (1)-(4). From the comparison, it can be seen that the static strengths obtained from the predicted and the FE results agree reasonably well for most models.

To provide quantitative estimation, error analyses are necessary to be carried out. Four errors, namely relative error, relative average error, relative standard deviation and average relative standard deviation, are presented and defined as follows

$$e_i^* = \frac{P_{fi} - P_{ci}}{P_{fi}} \qquad (i = 1, 2, 3 \ldots n) \tag{5}$$

$$e = \frac{\sum_{i=1}^{n} \left| e_i^* \right|}{n} \tag{6}$$

$$s^* = \sqrt{\frac{\sum_{i=1}^{n} \left| e_i^* \right|^2}{n-1}} \tag{7}$$

$$s = \sqrt{\frac{\sum_{i=1}^{n} \left(\left| e_i^* \right| - e \right)^2}{n-1}} \tag{8}$$

where P_{fi} and P_{ci} represent the static strengths for model i, and they are obtained from FE simulation and parametric equations respectively. n is the total number of the models used in the curve fitting process.

Through Eqs. (5)-(8), the accuracy of the presented parametric equations in predicting the static

strength of a collar-plate reinforced tubular T-joint is verified through error analyses. For Eqs. (1)-(2) for predicting the static strength of a collar-plate reinforced tubular T-joint under axial compression, the values of e, s* and s are 4.94%, 6.83%, and 4.48% respectively. Accordingly, for Eqs. (3)-(4) for predicting the static strength of a collar-plate reinforced tubular T-joint under axial tension, the values of e, s* and s are 6.32%, 8.6%, and 5.85% respectively. Such small errors show that Eqs. (1)-(4) are reliable and accurate to estimate the static strength of a collar-plate reinforced tubular T-joint under axial compression or tension.

As Eqs. (1)-(4) are obtained from curve fitting technique, the values of the parameters in these equations are necessary to be valid in a specified range, and the range is defined as follows: $0.2 \leq \beta \leq 0.8$, $12 \leq \gamma \leq 30$, $0.8 \leq \tau_c \leq 1.5$, $1.5 \leq l_c/d_1 \leq 2.5$.

6. Conclusions

From both experimental tests and FE simulations on collar-plate reinforced tubular T-joints under axial compression or tension, the following conclusions can be drawn:

- Experimental tests show that collar-plate can be used to improve the static strength of a tubular T-joint in remarkable efficiency.
- The failure mode of a collar-plate reinforced T-joint is dependent on the value of parameter β. Generally, the failure mode is local yielding when the value of β is small. However, the failure mode becomes the flexural yielding of the chord when the value of β is very big.
- Both β and γ have remarkable effect on improving the static strength of a collar-plate reinforced T-joint. Additionally, the thickness and the length of the collar-plate also show significant influence on improving the static strength.
- A set of parametric equations are presented for predicting the static strength of a collar-plate reinforced tubular T-joint under axial compression or tension. The reliability and accuracy of these equations are evaluated through error analyses.

Acknowledgments

This research work is supported by the National Natural Science Foundation (No. 50808153), and such support is appreciated by the authors.

References

Aguilera, J. and Fam, A. (2013), "Retrofitting tubular steel T-joints subjected to axial compression in chord and brace members using bonded FRP plates or through-wall steel bolts", *Eng. Struct.*, **48**, 602-610.

Chen, X.X., Chen, Y. and Wang, J. (2015), "Plate reinforced square hollow section X-joints subjected to in-plane moment", *J. Central South U.*, **22**(3), 1002-1015.

Chiew, S.P., Zhang, J.C., Shao, Y.B. and Qiu, Z.H. (2012), "Experimental and numerical analysis of complex welded tubular DKYY-joints", *Adv. Struct. Eng.*, **15**(9), 1573-1582.

Choi, B.J., Lee, E.T., Yang, J.G. and Kang, C.K. (2012), "Axial capacity of circular hollow section T-joints using grade HSB 600 steel", *Int. J. Steel Struct.*, **12**(4), 483-494.

Choo, Y.S., Li, B.H., Liew, J.Y.R. and van der Vegte, G.J. (1998), "Static strength of T-joints reinforced with doubler or collar plates", *Proceedings of the 8th International Symposium on Tubular Structures*,

Singapore, August, pp. 139-145.
Choo, Y.S., Liang, J.X. and van der Vegte, G.J. (2004a), "Static strength of doubler plate reinforced CHS X-joints loaded by in-plane bending", *J. Constr. Steel Res.*, **60**(12), 1725-1744.
Choo, Y.S., Liang, J.X., van der Vegte, G.J. and Liew, J.Y.R. (2004b), "Static strength of collar plate reinforced CHS X-joints loaded by in-plane bending", *J. Constr. Steel Res.*, **60**(12), 1745-1760.
Choo, Y.S., van der Vegte, G.J., Zettlemoyer, N. and Li, B.H. (2005), "Static strength of T-joints reinforced with doubler or collar plates-part I: experimental investigations", *J. Eng. Struct.*, ASCE, **131**(1), 119-128.
Fung, T.C., Chan, T.K. and Soh, C.K. (1999), "Ultimate capacity of doubler plate reinforced tubular joints", *J. Eng. Struct.*, ASCE, **125**(8), 891-899.
Gandhi, P., Raghava, G. and Ramachandra Murthy, D.S. (2000), "Fatigue behaviour of internally ring-stiffened welded steel tubular joints", *J. Eng. Struct.*, ASCE, **126**(7), 809-815.
Gao, F., Guan, X.Q., Zhu, H.P. and Xia, Y. (2015), "Hysteretic behaviour of tubular T-joints reinforced with doubler plates after fire exposure", *Thin Wall. Struct.*, **92**, 10-20.
Ghazijahani, T.G., Jiao, H. and Holloway, D. (2015), "Fatigue experiments on circular hollow sections with CFRP reinforced cutouts", *J. Constr. Steel Res.*, **106**, 322-328.
Hamid, A. and Esmaeil, Z. (2015), "Stress concentration factors induced by out-of-plane bending loads in ring-stiffened tubular KT-joints of jacket structures", *Thin-Wall. Struct.*, **91**, 82-95.
Hamid, A., Mohammad, A.L.-Y. and Shao, Y.B. (2013), "Chord-side SCF distribution of central brace in internally ring-stiffened tubular KT-joints: A geometrically parametric study", *Thin-Wall. Struct.*, **70**, 93-105.
Hamid, A., Amir, H.M. and Ali, Y. (2015), "Probability density functions of SCFs in internally ring-stiffened tubular KT-joints of offshore structures subjected to axial loading", *Thin-Wall. Struct.*, **94**, 485-499.
Hoon, K.H., Wong, L.K. and Soh, A.K. (2001), "Experimental investigation of a doubler-plate reinforced tubular T-joint subjected to combined loadings", *J. Constr. Steel Res.*, **57**(9), 1015-1039.
Jin, Y.F. and Shao, Y.B. (2010), "Hysteretic analysis of circular tubular T-joints with chord reinforcement", *J. Huazhong U.*, **27**(2), 78-81.
Kim, I.G., Chung, C.H., Shim, C.S. and Kim, Y.J. (2014), "Stress concentration factors of N-joints of concrete-filled tubes subjected to axial loads", *Int. J. Steel Struct.*, **14**(1), 1-11.
Lesani, M., Bahaari, M.R. and Shokrieh, M.M. (2013), "Numerical investigation of FRP-strengthened tubular T-joints under axial compressive loads", *Compos. Struct.*, **100**, 71-78.
Li, T., Shao, Y.B. and Zhang, J.C. (2009), "Study on static strength of tubular joints reinforced with horizontal inner plate", *Steel Constr.*, **24**(123), 25-29.
Lu, L.H., de Winkel, G.D., Yu, Y. and Wardenier, J. (1994), "Deformation limit for the ultimate strength of hollow section joints", *Proceedings of the 6th International Symposium on Tubular Structures*, Melbourne, Australia, December, p. 341-348.
Pena, A. and Chacon, R. (2014), "Structural analysis of diamond bird-beak joints subjected to compressive and tensile forces", *J. Constr. Steel Res.*, **98**, 158-166.
Shao, Y.B., Zhang, J.C., Qiu, Z.H. and Shang, J.J. (2009), "Strength analysis of large-scale multiplanar tubular joints with inner-plate reinforcement", *Int. J. Space Struct.*, **24**(3), 161-177.
Shao, Y.B., Li, T., Lie, S.T. and Chiew, S.P. (2011), "Hysteretic behaviour of square tubular T-joints with chord reinforcement under axial cyclic loading", *J. Constr. Steel Res.*, **67**(1), 140-149
Thandavamoorthy, T.S., Madhava Rao, A.G. and Santhakumar, A.R. (1999), "Behavior of internally ring-stiffened joints of offshore platforms", *J. Eng. Struct.*, ASCE, **125**(11), 1348-1352.
Van der Vegte, G.J., Choo, Y.S., Liang, J.X., Zettlemoyer, N. and Liew, J.Y.R. (2005), "Static strength of T-joints reinforced with doubler or collar plates, II: numerical simulations", *J. Eng. Struct.*, *ASCE*, **131**(1), 129-139.
Wang, C.Y., Chen, Y., Chen, X.X. and Chen, D.F. (2015), "Experimental and numerical research on out-of-plane flexural property of plates reinforced SHS X-joints", *Thin-Wall. Struct.*, **94**, 466-477.
Yin, Y., Han, Q.H., Bai, L.J., Yang, H.D. and Wang, S.P. (2009), "Experimental study on hysteretic behaviour of tubular N-joints", *J. Constr. Steel Res.*, **65**(2), 326-334.

Zhang, F., Chen, Y.J. and Chen, Y.Y. (2004), "Effects of ring-stiffeners on the behaviour steel tubular joints", *Spatial Struct*., **10**(1), 51-56.
Zhu, L., Zhao, Y., Li, S.W., Huang, Y.X. and Ban, L.R. (2014), "Numerical analysis of the axial strength of CHS T-joints reinforced with external stiffeners", *Thin-Wall*. *Struct*., **85**, 481-488.

BU